

Pushing the boundaries of chemistry? It takes #HumanChemistry

Make your curiosity and talent as a chemist matter to the world with a specialty chemicals leader. Together, we combine cutting-edge science with engineering expertise to create solutions that answer real-world problems. Find out how our approach to technology creates more opportunities for growth, and see what chemistry can do for you at:

evonik.com/career





Autonomous Self-Healing Elastomers with Unprecedented Adhesion Force

Zhen Zhang, Natasha Ghezawi, Bingrui Li, Sirui Ge, Sheng Zhao, Tomonori Saito,* Diana Hun,* and Peng-Fei Cao*

Self-healable elastomers are extremely attractive due to their ability to prolong product lifetime. An additional function that could further expand their applications is strong adhesion force to clean and dusty surfaces. This study reports a series of autonomous self-healable and highly adhesive elastomers (ASHA-Elastomer) that are fabricated via a simple, efficient, and scalable process. The obtained elastomers exhibit outstanding mechanical properties with elongation at break up to 2102% and toughness (modulus of toughness) of 1.73 MJ m⁻³. The damaged ASHA-Elastomer can autonomously self-heal with full recovery of functionalities, and the healing process is not affected by the presence of water. The elastomers are found to possess an ultrahigh adhesion force up to 3488 N m⁻¹, greatly outperforming previously reported self-healing adhesive elastomers. Furthermore, the adhesion force of the ASHA-Elastomer is negligibly affected by dust on the surface, in stark contrast with regular adhesive polymers that have adhesion strengths extremely sensitive to dust. The successful development of high-toughness, autonomous self-healable, and ultra-adhesive elastomers will enable a wide range of applications with enhanced longevity and versatility, including their use in sealants, adhesives, and stretchable devices.

1. Introduction

High-performance elastomers are widely used in various applications including automotive, building construction, and flexible electronics/devices.^[1–8] Improving their performance and longevity will not only expand their applications but also help conserve natural resources towards sustainable future. In human skin, minor cuts can completely heal over time and the operational capability as well as sensory functionalities is typically restored even after severe injuries. Elastomers that have similar self-healing capabilities will be a significant

improvement over current technologies as they provide a much longer lifetime.^[9–12] Various methodologies have been developed for the preparation of self-healing elastomers. One approach utilizes extrinsic self-healing through encapsulating healing agents,[13-16] which typically is a singular healable process in a given location. Another approach uses intrinsic self-healing achieved by physical interactions or dynamic covalent bonds, providing the advantage of multicycle recoverability.[17-22] A main limitation of most of the intrinsic self-healing processes is that they require an external stimulus, such as heat,[23-28] light,[29-31] or pressure^[32,33] to reestablish the properties after initial damage. The need for a stimulus makes these intrinsic self-healing materials impractical and thus limits their applications especially in the areas of buildings, aerospace, deep-sea exploration, and aerial work, given the extra cost, risk, or difficulty to reach the fractured

locations. Consequently, autonomous intrinsic self-healing elastomers are highly desirable for a wide range of applications.

Self-healing elastomers that have outstanding mechanical properties and promising functionalities have been successfully demonstrated. However, adhesion force in these self-healing elastomers has been minimally addressed, although this additional function could significantly increase their areas of application. Self-healing elastomers with high adhesion is particularly important in applications such as artificial skins, wearable electronics, and sealants, in which close contact of the functional moieties with the stretchable substrates is critical throughout the

Dr. Z. Zhang, N. Ghezawi, Dr. T. Saito, Dr. P.-F. Cao Chemical Sciences Division Oak Ridge National Laboratory Oak Ridge, TN 37830, USA E-mail: saitot@ornl.gov; caop@ornl.gov N. Ghezawi, B. Li, Dr. T. Saito

Bredesen Center for Interdisciplinary Research and Graduate Education University of Tennessee Knoxville, TN 37996, USA

The ORCID identification number(s) for the author(s) of this article can be found under https://doi.org/10.1002/adfm.202006298.

DOI: 10.1002/adfm.202006298

B. Li, S. Zhao Department of Chemistry University of Tennessee Knoxville, TN 37996, USA

Dr. D. Hun

S. Ge
Department of Materials Science and Engineering
University of Tennessee
Knoxville, TN 37996, USA

Buildings and Transportation Science Division Oak Ridge National Laboratory Oak Ridge, TN 37830, USA E-mail: hunde@ornl.gov





www.afm-journal.de

entire life of the product.[1,41-45] For example, for the wearable strain sensors reported by Zeng et al., close and long-lasting contact with human skin is crucial to accurately detect human activities and any detachment from the skin could lead to functionality failure. [41] At the same time, the self-healability automatically repairs cracks that may develop over time, which will increase the products' lifetime. Till now, several elastomers have been reported to simultaneously display self-healing and adhesive properties, but most of them exhibit significant limitations, such as low adhesion strength, weak mechanical performance, or strong adhesion only to specific substrates. [46–48] For example, self-healing polymers based on 2-ureido-4[1H]-pyrimidinone (UPy)[47] exhibited some adhesive property owning to the presence of strong quadruple-hydrogen-bonding UPy units.[49,50] However, their adhesion strength is too weak (<1 N m⁻¹) to have practical applications. Notable progress was made by Hayes and co-workers in 2016 as they synthesized a polyurethane-based elastomer capable of fully self-healing at body temperature and achieved strong adhesion to animal skin (peel strength of 1600 N m⁻¹).^[46] More recently, Tian et al. reported a poly(thioctic acid)-based self-healing supramolecular polymer with high adhesion strength, although adhesion was only evaluated by shear strength measurement of the polymer sandwiched between two substrates.^[51] Novel material designs are needed to make self-healing elastomers more feasible in the areas where strong adhesion is critical.

We report here a series of autonomously self-healable, highly adhesive elastomers (ASHA-Elastomers) that were prepared using a synthetic self-healing polymer and curable elastomers. The self-healing process of the developed ASHA-Elastomers is autonomous and intrinsic, that is, they do not require external stimuli or encapsulated chemicals. Mechanical properties are fully recovered after self-healing process at ambient condition or under water, which is comparable to most of state-of-the-art selfhealable materials. [52-55] Most notably, unlike regular adhesive elastomers with adhesion always greatly impaired by the dust on the substrates, the ASHA-Elastomers display comparable adhesion on both clean and dusty surface with adhesion force up to 3500 N m⁻¹, which greatly surpasses the bonding strength of tendon and cartilage to bone in many animals (800 N m⁻¹). [56,57] To the best of our knowledge, this adhesion value significantly exceeds the currently reported adhesive self-healing elastomers, and the development of materials possessing autonomous selfhealing and ultra-adhesion force provides an extremely meaningful path for a wide range of applications.

2. Results and Discussion

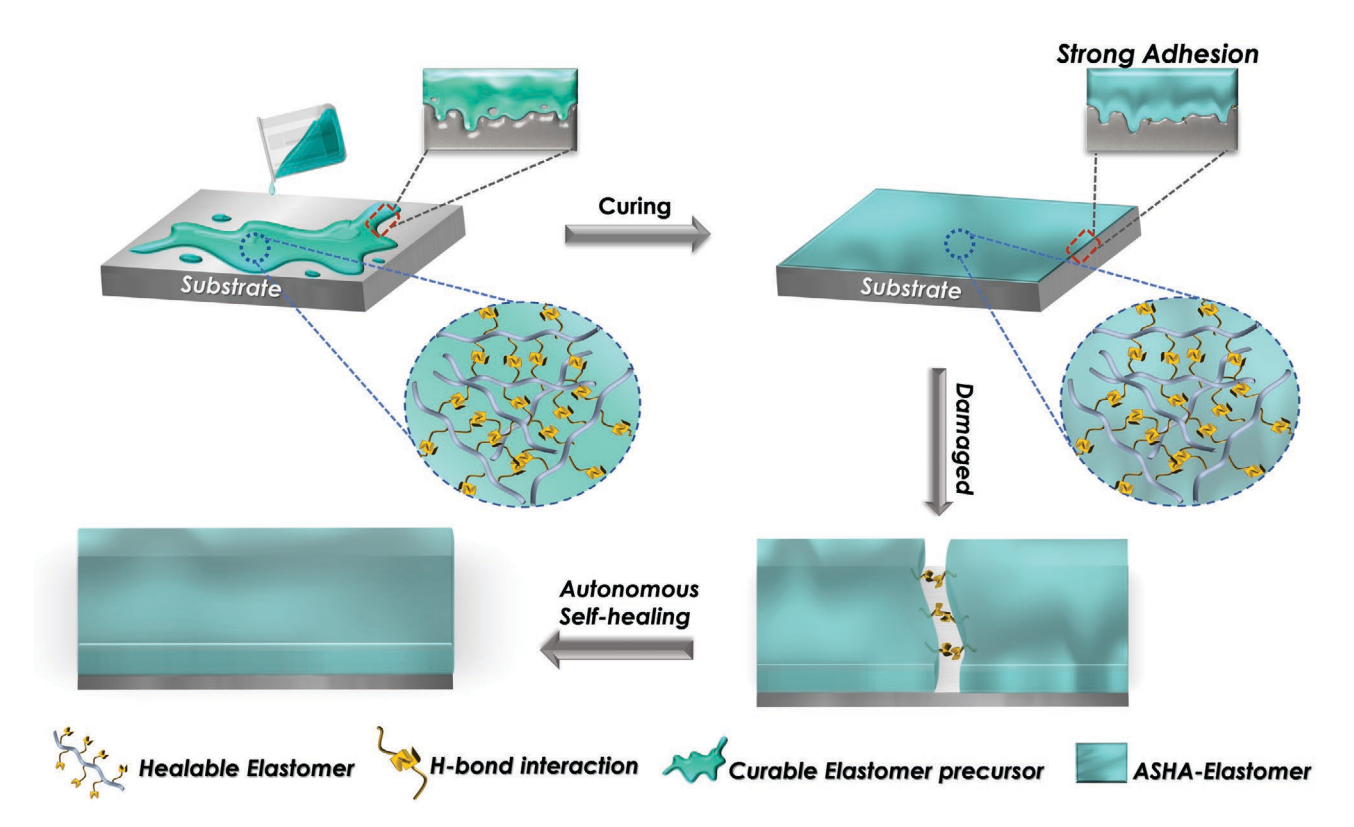
2.1. Preparation of ASHA-Elastomers

The designed ASHA-Elastomers are composed of self-healable poly(2-[[(butylamino)carbonyl]oxy]ethyl acrylate) (Poly(BCOE)) and curable elastomer (C-Elastomer) as depicted in **Scheme 1**. Poly(BCOE) was synthesized through a single-step radical polymerization from 2-[[(butylamino)carbonyl]oxy]ethyl acrylate (BCOE) monomers, and the chemical structure of Poly(BCOE) was confirmed with the ¹H NMR spectrum (**Figure 1**). The obtained Poly(BCOE) exhibits excellent extensibility with elongation at break of more than 3000%. The low glass transition

temperature ($T_g \approx -3$ °C) and hence fast segmental dynamics at ambient temperature along with the numerous sacrificial hydrogen bonds of urethane groups (circled in Figure 1) introduced the self-healing property to the obtained elastomer system. The C-Elastomers, including silicon-based elastomers, i.e., C1-Elastomer and C2-Elastomer, and polyurethanebased elastomer, i.e., C3-Elastomer, generate high adhesive force due to the following two processes: 1) good contact of the elastomer precursors (liquid-like) with the substrate; and 2) the subsequent moisture-triggered chemical cross-linking process^[58,59] that leads to formation of high-toughness elastomers. Poly(BCOE) and C-Elastomers were mixed at a temperature of 40-50 °C and subsequently applied to several substrates, after which the obtained ASHA-Elastomer precursors were allowed to cure at 30 °C for 1 week. By varying the weight ratio of Poly(BCOE) and C-Elastomers from 1:9 to 3:7 and eventually to 5:5, a series of self-healable, highly-adhesive elastomers, namely ASHA-C-Elastomers-n (C is the type of curable elastomer, n is the weight percentage of Poly(BCOE)), were produced (see detailed procedure in Experimental Section). The characteristic chemical structures were revealed by infrared (IR) spectroscopy as shown in Figure 2A and Figure S1, Supporting Information. Peaks at ≈3340, ≈1700, and ≈1530 cm⁻¹ correspond to N-H stretching, C=O stretching, and N-H bend, respectively, of which the intensity are gradually enhanced from top to bottom, owning to the increased contents of Poly(BCOE). The obtained elastomers exhibit good thermostability with no weight loss observed up to 250 °C (Figure S2, Supporting Information). Differential scanning calorimetry (DSC) (Figure 2B) curve of ASHA-C1-Elastomer displays melting temperature $(T_{\rm m})$ at -45 °C and $T_{\rm g}$ at -3 °C, originating from silicon-based C1-Elastomer and Poly(BCOE), respectively. Clear presence of the T_{σ} from Poly(BCOE) along with its unshifted position in the DSC curve of the ASHA-C1-Elastomer indicates the presence of multiphases in the obtained elastomers. In the meanwhile, no significant peaks observed in the small-angle X-ray scattering (SAXS) spectrum of ASHA-C1-Elastomer-50 demonstrate the absence of long-range ordered phase behavior in the ASHA-C1-Elastomer (Figure S4, Supporting Information), which is in contrast with block copolymer systems that show ordered phase behavior. [60,61] This phase behavior could be critical for the materials to synergistically inherit the properties from both components and improve the overall performance, as observed in other multicomposite polymer systems. [62,63]

2.2. Mechanical Properties

The mechanical properties of the designed elastomers are critical to various applications, and they can be probed through their viscoelasticity. Therefore, rheometer was first used to evaluate the viscoelastic behaviors of the ASHA-C1-Elastomers with different weight ratios of Poly(BCOE) as shown in Figure 3A. The ASHA-C1-Elastomers show more solid-like (elastic modulus (G') > loss modulus (G'')) behavior over the frequency range at ambient temperature, which indicates mechanical robustness of the elastomers.^[35] Compared with the high G' value of the C1-elastomer, the G' values of ASHA-C1-Elastomers decrease with the increased ratios of Poly(BCOE). This can be



Scheme 1. Demonstration of the strong adhesion formation of ASHA-Elastomer on aluminum substrate and its self-healing process through hydrogen bond interactions and molecular dynamics of the self-healable polymer Poly(BCOE).

explained by the gradually decreased cross-linking densities of ASHA-C1-Elastomers with increased ratio of Poly(BCOE). Moreover, as indicated by the closer values of G' curves and G'' curves, increasing the content of Poly(BCOE) confers a more liquid-like character on the ASHA-C1-Elastomers (i.e., faster

molecular dynamic), which is critical to maintain their self-healability and develop a high adhesion strength to dusty surfaces as discussed later. To study the temperature effect on the modulus, we performed dynamic mechanical analysis (DMA) as illustrated in Figure S5, Supporting Information. Compared

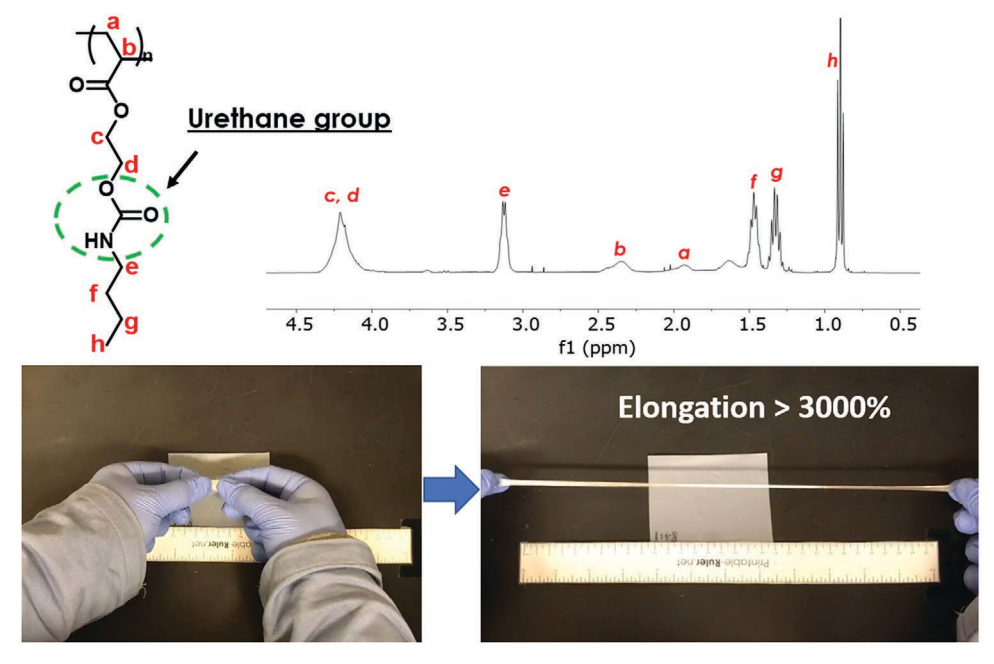
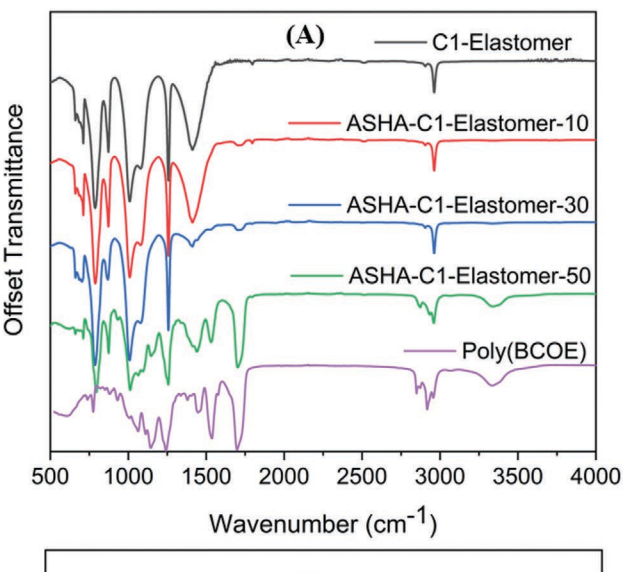


Figure 1. Chemical structure, ¹H NMR, and elasticity demonstration of Poly(BCOE).



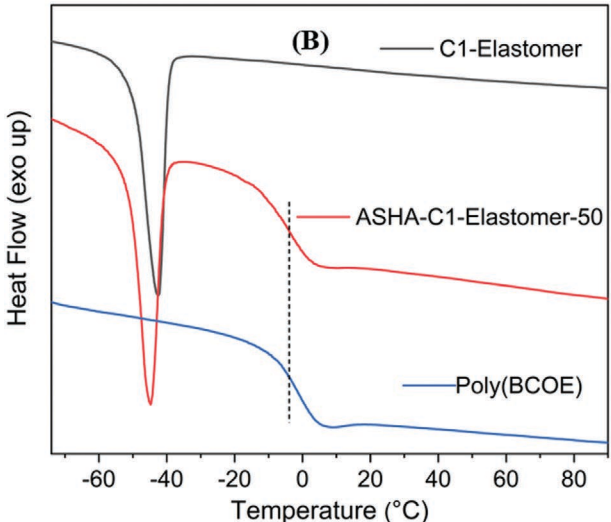


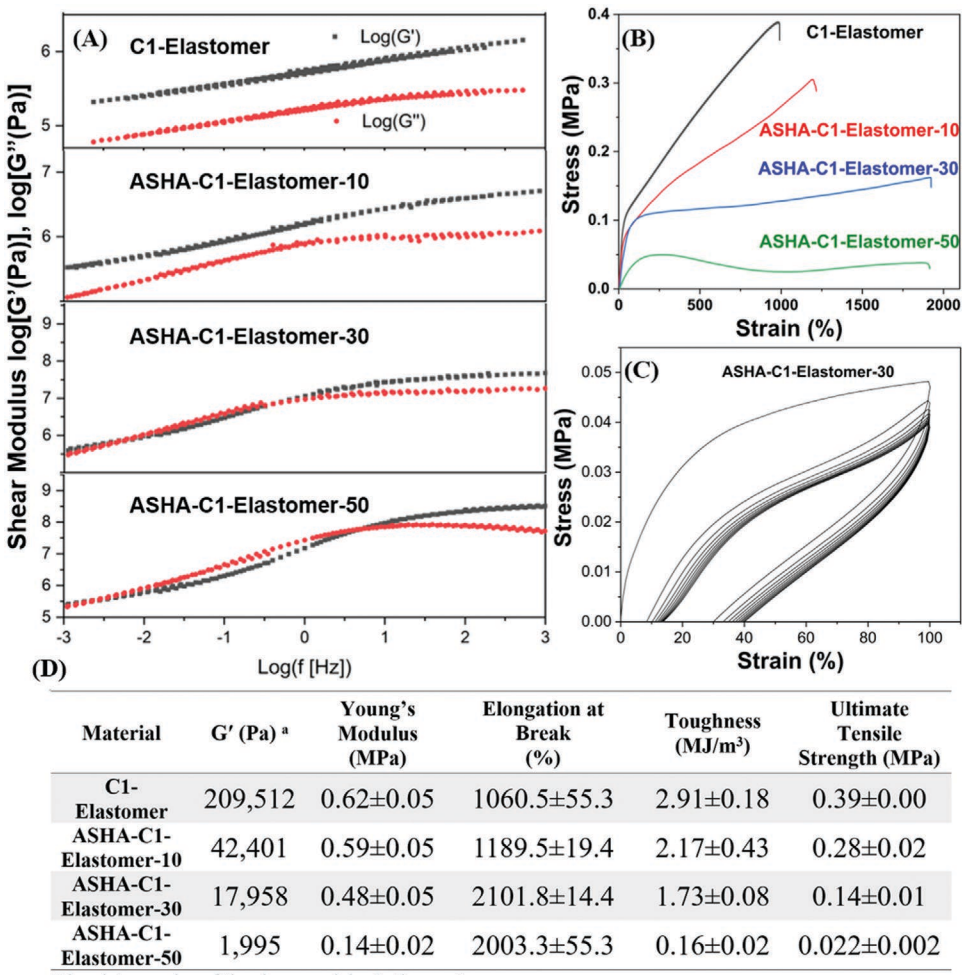
Figure 2. A) IR spectroscopy of curable elastomer (C1-Elastomer), self-healable polymer (Poly(BCOE)), and ASHA-C1-Elastomers with different weight ratios. B) DSC curves of the C1-Elastomer, ASHA-C1-Elastomers-50, and Poly(BCOE).

to the C1-Elastomer, the addition of Poly(BCOE) increased both G' and G" of ASHA-C1-Elastomers at temperature below 0 °C due to the glassy state of Poly(BCOE). The modulus experienced a gradual drop from 0 to 40 °C, which is essential to the efficient recovery of mechanical properties at temperature above 0 °C as demonstrated later. Mechanical properties of the elastomers were also investigated through tensile tests as shown in Figure 3B,D. Compared with other reported self-healable adhesive elastomers, [41,46,48,51,64–67] the designed ASHA-C1-Elastomers exhibit either comparable or higher mechanical performance in terms of Young's modulus, extensibility, and ultimate tensile strength. All of the ASHA-C1-Elastomers display great extensibility with elongation at break higher than 1000%, which can be further enhanced to 2000% by increasing the weight ratio of Poly(BCOE). Both Young's modulus and ultimate tensile strength of the ASHA-C1-Elastomers gradually decreased with increased ratio of Poly(BCOE) due to the reduced cross-linking

density, which is consistent with the rheology measurements. The overall toughness of ASHA-C1-Elastomer-10 and ASHA-C1-Elastomer-30 is comparable, which can be explained that the "sacrificial" noncovalent interactions from Poly(BCOE) compensate for the dissipation energy loss with lower chemical cross-linking density in the system. [68] In order to investigate the effects of Poly(BCOE) on the properties of other elastomeric systems and enlarge the library of this type of adhesive self-healing materials, ASHA-Elastomers composed of C2-Elastomers or C3-Elastomers were also prepared following the same procedures with that of C1-Elastomer. Compared with ASHA-C1-Elastomers, ASHA-C2-Elastomers and ASHA-C3-Elastomers generally exhibited improved Young's modulus, toughness, and ultimate tensile strength (Tables S1 and S2, Supporting Information). They showed elongation at break in the range of 500-1000%, which is relatively lower than that of ASHA-C1-Elastomers but still better compared to most of the reported adhesive self-healing elastomers. [46,64,65] The elastic recovery of ASHA-Elastomers was investigated by applying 10 cycles of 0-100% strain as shown in Figure 3C. They display good elastic recovery, for example, the remaining stress of ASHA-C1-Elastomer-30 after 10 cycles can still maintain 83.3% of the initial value (40 vs 48 kPa) at 100% strain. The hysteresis observed for the elastomer may be caused by the presence of physical interactions between Poly(BCOE)s that can dissipate energy during stretching.

2.3. Self-Healing Properties

Integrating autonomously self-healing capability into highperformance elastomers is a promising way to boost the overall product functionalities and prolong their lifetime.^[9,41] Therefore, the self-healing efficiencies of the ASHA-Elastomers were investigated by evaluating the recovery of their mechanical and barrier properties through tensile measurements and ink permeation tests (Figure 4). The ASHA-Elastomer samples were either completely cut into two halves or partially (≈50%) cut to mimic microcracks that may develop as products age, after which the damaged parts from the fully-cut samples were placed side by side and let self-heal at ambient conditions for 2 days. The control samples (i.e., intact samples) were also kept under the same conditions before testing. With 10 wt% of Poly(BCOE), the ASHA-C1-Elastomer-10 exhibited negligible self-healability after being completely cut, perhaps due to the limited amount of physical-interaction units in the elastomer. With increased percentage of Poly(BCOE), ASHA-C1-Elastomer-30 ASHA-C1-Elastomer-50 showed excellent self-healing capability (Figure 4C), which is attributable to the presence of large amounts of H-bonds and their fast molecular dynamics at ambient temperature. Mechanical parameters including Young's modulus, elongation at break, and ultimate tensile strength of the half-way-cut samples completely recovered after 2 day healing process at ambient conditions (20 °C) for these elastomers. However, when it comes to the completely cut samples, the mechanical parameters of ASHA-C1-Elastomer-30 did not completely recover. For example, the elongation at break dropped from 2102% for the control sample to 684% for the self-healed sample. By increasing the Poly(BCOE) content to

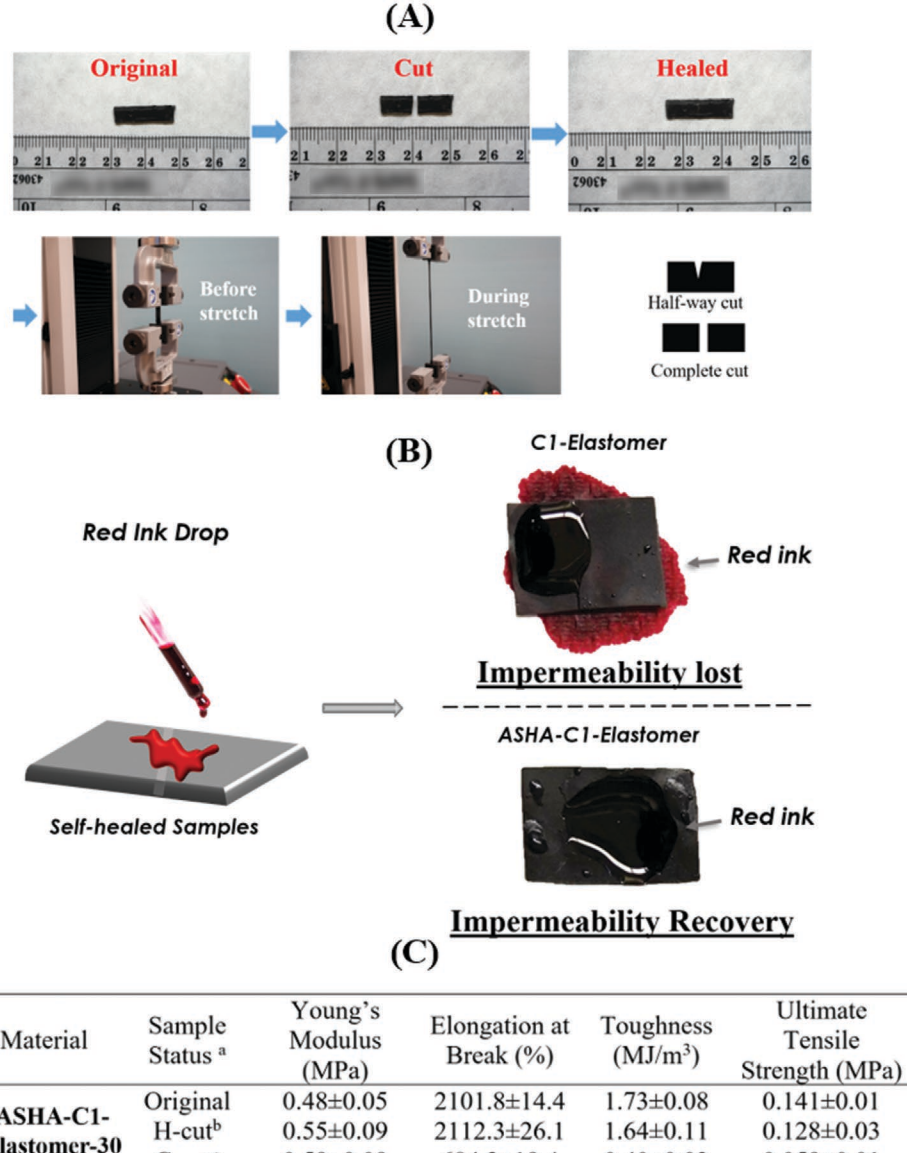


a the plateau value of the shear modulus in the master-curve.

Figure 3. A) Shear modulus (G' and G'') and B) tensile tests of ASHA-C1-Elastomers. C) Ten successive loading–unloading cycles of the film prepared from ASHA-C1-Elastomer-30. D) Mechanical properties of ASHA-C1-Elastomers.

50 wt%, the ASHA-C1-Elastomer-50 can completely self-heal as indicated by the fully recovered toughness. Depending on the specific requirements for mechanical robustness and selfhealing efficiency in different applications, both ASHA-C1-Elastomer-30 and ASHA-C1-Elastomer-50 are potentially useful. Self-healing efficiency of the ASHA-C1-Elastomers was further evaluated with an ink penetration test as shown in Figure 4B. The samples were cut and healed under the same previously described conditions. It was clearly noticed that the red ink easily went through the damaged area of the control sample that lacked Poly(BCOE), indicating loss of impermeability after damage. In contrast, ASHA-C1-Elastomer-50 exhibited impermeability after the self-healing process as red ink did not penetrate the damaged area, which again demonstrated the excellent self-healing performance of the ASHA-Elastomers. It is noticed that the ASHA-Elastomers need 2 days (Figure S6, Supporting Information) for complete recovery of mechanical performance, which is comparable to most of the self-healing materials^[52–55] and slightly longer than a few self-healable materials.^[69] This observation is reasonable given that the self-healable component Poly(BCOE) only takes up to 50 wt% of the ASHA-Elastomers, and the main component is a cross-linked polymeric system, which may suppress the fast dynamic of Poly(BCOE) and lead to slightly longer self-healing time. Notably, self-healing at the same location can be repeated at least three times with minimal effect on mechanical properties as shown in Figure S7, Supporting Information, which is a great advantage of intrinsic self-healing polymeric materials. To investigate the effect of temperature, the efficiency of the self-healing process was tested at low (i.e., 0 °C) and high (i.e., 40 °C) temperatures as shown in Figure S8, Supporting Information. At 0 °C, the elastomer heals much slower with around 80% toughness recovered in 1 week, due to the suppressed molecular dynamics of Poly(BCOE) at temperatures that are close to its T_g (-3 °C). In contrast, at 40 °C, much shorter time, i.e., 12 h, is required to let the elastomer completely self-heal, due to the enhanced molecular dynamics at elevated temperatures.

For the products that apply in automotives, outdoors, or even human body (flexible electronics), water or high humidity is always an inevitable factor that usually adversely affect their self-healing performance.^[70] Therefore, the healing efficiency in the presence of water was investigated. ASHA-C1-Elastomer-50



Material	Sample Status ^a	Young's Modulus (MPa)	Elongation at Break (%)	Toughness (MJ/m³)	Ultimate Tensile Strength (MPa)
ASHA-C1- Elastomer-30	Original H-cut ^b	0.48±0.05 0.55±0.09	2101.8±14.4 2112.3±26.1	1.73±0.08 1.64±0.11	0.141±0.01 0.128±0.03
	C-cut ^c	0.59 ± 0.09 0.59 ± 0.09	684.2±19.4	0.40 ± 0.11	0.059 ± 0.01
ASHA-C1- Elastomer-50	Original	0.14 ± 0.02	2003.3±55.3	0.16 ± 0.02	0.022 ± 0.002
	H-cut	0.21 ± 0.01	1722.6 ± 22.1	0.20 ± 0.01	0.033 ± 0.005
	C-cut	0.11 ± 0.01	2196.6±53.5	0.22 ± 0.03	0.028 ± 0.004

a The elastomers were cured for one week at r.t. and healed for two days at ambient condition before testing; b healed after half-way cut; c healed after completely cut.

Figure 4. Pictures showing A) the healing process of ASHA-C1-Elastomer, the damaged sample was healed for 2 days at ambient condition before tensile test; B) ink tests for C1-Elastomer and the ASHA-C1-Elastomer-50 self-healed after completely cut; and C) tensile test results of the original samples and self-healed samples after half-way cut or completely cut.

was tested because of its encouraging self-healing performance. The completely cut samples were placed side by side and then submerged in a water-filled Teflon dish for 2 days at 20 °C before testing as shown in Figure S11, Supporting Information. Results indicate that the obtained mechanical parameters were comparable for the samples that self-healed under water and at ambient conditions, indicating the self-healing process of ASHA-Elastomers is insensitive to the presence of water.

2.4. Adhesive Properties

With the development of advanced materials, adhesion has been emerging as a key factor towards reliable product and significantly determines how well the other predesigned functionalities perform.[46,64,71] Combining the autonomously self-healability with high adhesion force is especially attractive since it can significantly improve the overall performance of elastomers towards

www.afm-journal.de

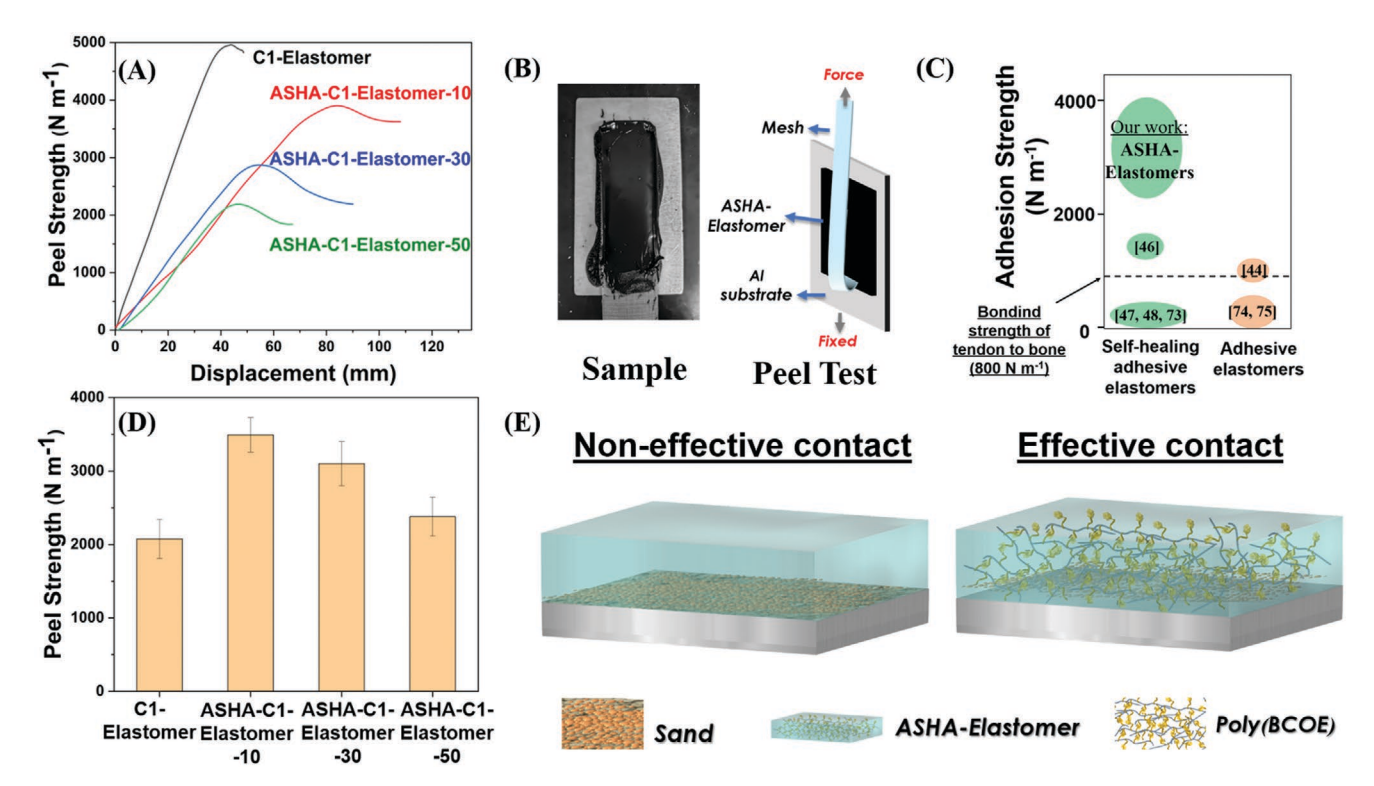


Figure 5. A) Peel tests of ASHA-C1-Elastomers. B) Picture and schematic illustration showing the prepared ASHA-Elastomers on Al substrate and the 180 °C peel test. C) Adhesion comparison of ASHA-Elastomers with reported values from corresponding literatures. D) Peel test results of ASHA-C1-Elastomers on dusty surface. E) Demonstration of the adhesion improvement of ASHA-C1-Elastomers on dusty surface caused by the encapsulation effect of Poly(BCOE).

a wide range of applications. Herein, adhesion properties of the ASHA-Elastomers were evaluated through peel adhesion tests (Figure 5A,B) on aluminum substrates following the ASTM C794 test standard; detailed description of sample preparation is in the Experimental Section. On clean aluminum substrates, C1-Elastomer exhibits a peel strength up to 4960 (±253) N m⁻¹ (Figure 5A). With the incorporation of Poly(BCOE), the peel strengths of ASHA-Elastomers slightly decrease (2187–4132 N m⁻¹) but are still far beyond the reported adhesive elastomers (1-1600 N m⁻¹) as illustrated in Figure 5C, [72-75] and are much higher than the bonding strength of tendon and cartilage to bone (800 N m⁻¹). Temperature effect on peel strength was evaluated on ASHA-C1-Elastomer-30 at 0, 20, and 40 °C as shown in Figure S9, Supporting Information. It was found that the ASHA-C1-Elastomer-30 exhibits stronger adhesion $(3502 \pm 238 \text{ N m}^{-1})$ at 0 °C than at 20 °C (2888 \pm 223 N m⁻¹), due to the increased modulus of the elastomer at temperatures that are close to the T_{g} of Poly(BCOE) (-3 °C) as indicated by the DMA measurement (Figure S5, Supporting Information). However, changes in adhesion force were not observed between 20 and 40 °C (2884 \pm 156 N m⁻¹) perhaps due to the absence of a state transition process at this temperature range.

Usually, a perfectly clean surface is difficult or sometimes impossible to prepare in practical deployment, which usually induces adhesion failure in traditional adhesives. [76,77] Therefore, it is of great importance for the newly designed materials to maintain the strong adhesion on dusty surface. Surprisingly, the ASHA-C1-Elastomers with self-healing capability even displayed stronger adhesion strength to dusty substrates than the curable elastomer (i.e., C1-Elastomer), which is opposite to the peel strength results that were obtained from clean substrates (i.e., lower peel strength of ASHA-C1-Elastomers vs. C1-Elastomer). For example, an adhesion force of 3488 N m⁻¹ was obtained from ASHA-C1-Elastomer-10 on dusty surface, which is about 68% higher than that of C1-Elastomer on a dusty substrate (2076 N m⁻¹). A possible explanation for the higher adhesion of ASHA-Elastomers on dusty surface is illustrated in Figure 5E. The presence of dust leads to reduced contact area and hence much weaker overall adhesion force between the C1-Elastomer and the substrate. In contrast, the ASHA-C1-Elastomers are able to "encapsulate" the dust particles due to the efficient physical interaction and fast polymer dynamic of Poly(BCOE) at ambient condition. Therefore, the adhesion force of ASHA-C1-Elastomers will not be significantly affected by dusty surfaces as shown in Figure 5D. Similarly, the adhesion improvement on dusty surfaces was also observed in ASHA-C2-Elastomers (Table S3, Supporting Information) and ASHA-C3-Elastomers (Table S4, Supporting Information), demonstrating the universality of our methodology. The high adhesion strength of the ASHA-Elastomers on dusty surfaces will be a significant improvement for technologies that need to be applied to surfaces that cannot be thoroughly cleaned.

The self-recovery efficiency of the adhesion force of damaged samples was also evaluated as demonstrated in Figure S10, Supporting Information. The peel test samples were cut in the direction parallel to the substrate (Figure S10a, Supporting





www.afm-iournal.de

Information) and then allowed to self-heal at room temperature. After 2 days, the peel test shows a 57% recovery of the adhesion force (1240 \pm 92 N m $^{-1}$) compared to that from the original sample (2184 \pm 131 N m $^{-1}$). The difference in recovery efficiency of the mechanical properties (100%) and adhesion force (57%) may be caused by the slight detachment of elastomers from the substrate during the cutting process for the adhesion recovery test.

3. Conclusion

We reported a series of ASHA-Elastomers exhibiting excellent mechanical properties, autonomous self-healability at ambient temperature, and ultra-strong adhesion force to substrate. The ASHA-Elastomers can be simply prepared from synthetic selfhealable Poly(BCOE) and commercially available curable elastomers. ASHA-Elastomers can reach elongation at break of \approx 2000% with overall toughness being 1.73 MJ m⁻³ as indicated by tensile tests. The ASHA-Elastomers display autonomous self-healability with completely recovered mechanical properties at ambient environment or underwater conditions, which will considerably extend a material's lifetime under various operational conditions. The ASHA-Elastomers possess ultrahigh adhesion strength on both clean (4132 N m⁻¹) and dusty (3488 N m⁻¹) substrates, which is much stronger than the bonding strength of tendon and cartilage to bone (800 N m⁻¹) in many animals and significantly exceeds previous reported self-healable adhesive elastomers (1–1600 N m⁻¹). Moreover, unlike curable elastomers that experience a sharp drop in adhesion force with the presence of dust, the adhesion force of ASHA-Elastomers is negligibly affected by the dust due to the "encapsulation" effect of the dynamic polymer, Poly(BCOE). With these outstanding mechanical properties, self-healing capabilities, and adhesion performance, the ASHA-Elastomer opens new opportunities to develop functional materials that could exceed the strict demands required by industries such as automotive, building construction, flexible electronics/devices, and others.

4. Experimental Section

Materials and Instruments: Commercial reactants and solvents were used without further purification unless otherwise noted. BCOE was filtered through inhibitor remover before polymerization with AIBN. C1-Elastomer (Dow790) and C2-Elastomer (Dow995) were purchased from Dow, Inc. C3-Elastomer (3M540) was purchased from 3M. The dust (MIL-STD-810G Blowing Dust) used for the peel study was purchased from Powder Technology, Inc. The particle size distribution was less than 150 microns, with a median diameter of 20 ± 5 microns. Particle size was determined using a laser diffraction analyzer. ¹H NMR spectra were recorded on a Bruker instrument (400 MHz) and internally referenced to the residual solvent signals of CDCl₃ for ¹H at 7.26 ppm. IR spectra were recorded on a Cary 600 Series FTIR spectrometer (Agilent Technologies). DSC measurements were performed on TA Instrument DSC2500 with ≈10 mg sample and at scan rates of 10 °C min⁻¹.

Synthesis of Poly(PBCOE): Ten grams of BCOE (46.5 mmol) and 15.2 mg of azobisisobutyronitrile (0.0926 mmol) were added into a round-bottom flask and dissolved in 20 mL of anhydrous dimethylformamide. After a 30 min of purge with nitrogen gas while

stirring, the solution was heated in an oil bath at 68 °C for 24 h. The crude product was precipitated in 300 mL of deionized water. The sticky white precipitate was collected and dissolved in ethyl acetate, then precipitated in 300 mL of hexane, after which the process was repeated two more times. The final product was then collected in a Teflon dish and the leftover organic solvent was removed by placing the product in a vacuum oven for 48 h.

Preparation of ASHA-Elastomer: Poly(BCOE) was transferred into a small Teflon dish with a diameter of 7 cm and weighed out. Then the curable elastomer precursor with desirable amount was weighed out in the same Teflon dish. Keeping each part of the mixture on two sides of the dish, the Poly(BCOE) was heated with a heat gun and mixed with C1, C2, or C3-Elastomer precursors. The moisture-triggered curing process occurred at ambient condition, and the preparation described below was performed immediately after making the blend.

Samples for Tensile Analysis: Five grams of Poly(BCOE)/sealant mixture was spread on a Teflon sheet at a thickness of 2 mm. After curing for 1 week, the sample was cut into 7 mm \times 40 mm strips. For the self-healing samples, the strips were taken and cut either halfway or completely and placed side-by-side, which was left under ambient condition for 2 days. The samples were tested with the Instron 3343 Universal Testing System following the ASTM D1708 standard, and the reported tensile data are an average of three samples.

Rheology Measurement: The viscoelastic properties of the ASHA-Elastomers were probed by small amplitude oscillatory shear measurements through a strain-controlled mode of the AR2000ex (TA Instruments) in an angular frequency range of 10^{-1} – 10^2 rad s⁻¹ using parallel plate geometry, with a disk diameter of 4 mm. The gap between plates was about 1 mm for all the samples. Before each measurement, the sample was annealed at 100 °C for 10 min to remove the thermal history. Then the sample was quenched to temperature near $T_{\rm g}$ before frequency sweep was conducted at different temperatures. Prior to each frequency sweep measurement, the sample underwent thermal stabilization for 5 min to make sure that thermal equilibrium had reached.

Dynamic Mechanical Analysis: Hysteresis analysis was performed on a TA Instruments RSA-G2 Solids Analyzer. Sample preparation is the same as that for tensile analysis, and films were cut into $\approx\!18.0\times5.0\times0.5$ mm specimens. Samples were elongated to 100% strain and then back to 0% strain at a constant rate of 1 mm s $^{-1}$, ten cycles of testing were performed for each sample.

Samples for Peel Test: Two different aluminum molds were prepared: one with a thickness of 2 mm and the other with a thickness of 4 mm. A 50.8 mm \times 76.2 mm \times 1.27 mm aluminum substrate was used for peel test of each sample. The aluminum plate was taped at the bottom and the 2 mm thick mold was placed on top. Half of the mixture was placed on the substrate and smoothed out evenly using the mold. A 23 mm strip of 304 McMaster-Carr Stainless Steel Wire Cloth with 100 \times 100 mesh size and 0.0055 opening size was then embedded on the placed mixture followed by replacing the 2 mm thick mold with a 4 mm thick mold. The rest of the mixture was placed on the embedded wire mesh and spread evenly, making the entire specimen 4 mm thick. The sample was cured for 1 week at 30 °C and then tested with the universal testing machines following the ASTM C794 test standard. Picture illustrations of each step are included in the Supporting Information (Figure S12, Supporting Information).

Samples for Dust Test: A 50.8 mm \times 76.2 mm \times 1.27 mm aluminum plate was submerged in a container of MIL-STD-810G Blowing Dust for 4 h before sample preparation. The average amount of blowing dust on each aluminum plate was around 54.5 mg. After the plate was dusted, the peel test preparation above was followed.

Supporting Information

Supporting Information is available from the Wiley Online Library or from the author.



www.afm-journal.de

Acknowledgements

Z.Z. and N.G. contributed equally to this work. This work was funded by the U.S.-China Clean Energy Research Center for Building Energy Efficiency (CERC BEE) under the Building Technologies Office (BTO) of the U.S. Department of Energy (DOE), under contract no. DE-ACO5-00OR22725. This manuscript was authored by UT-Battelle, LLC under contract no. DE-ACO5-00OR22725 with the U.S. Department of Energy. The United States Government retains and the publisher, by accepting the article for publication, acknowledges that the United States Government retains a non-exclusive, paid-up, irrevocable, worldwide license to publish or reproduce the published form of this manuscript, or allow others to do so, for United States Government purposes. The Department of Energy will provide public access to these results of federally sponsored research in accordance with the DOE Public Access Plan (http://energy.gov/downloads/doe-public-access-plan).

Conflict of Interest

The authors declare no conflict of interest.

Keywords

autonomous self-healing, elastomer, hydrogen bonding, strong adhesion

Received: July 26, 2020 Revised: September 29, 2020 Published online: October 14, 2020

- J. Kang, D. Son, G. J. N. Wang, Y. Liu, J. Lopez, Y. Kim, J. Y. Oh, T. Katsumata, J. Mun, Y. Lee, Adv. Mater. 2018, 30, 1706846.
- [2] S. Liu, S. Wang, S. Xuan, S. Zhang, X. Fan, H. Jiang, P. Song, X. Gong, ACS Appl. Mater. Interfaces 2020, 12, 15675.
- [3] M. A. Hickner, H. Ghassemi, Y. S. Kim, B. R. Einsla, J. E. McGrath, Chem. Rev. 2004, 104, 4587.
- [4] Z. Wei, S. Thanneeru, E. M. Rodriguez, G. Weng, J. He, Soft Matter 2020, 16, 2276.
- [5] X. Zhou, L. Wang, Z. Wei, G. Weng, J. He, Adv. Funct. Mater. 2019, 29, 1903543.
- [6] K. Zhang, P. Froimowicz, L. Han, H. Ishida, J. Polym. Sci., Part A: Polym. Chem. 2016, 54, 3635.
- [7] J. Moon, S. B. Kwak, J. Y. Lee, J. S. Oh, *Elastomers Compos.* **2017**, *52*, 249.
- [8] H. Özen, A. Aksoy, S. Tayfur, F. Çelik, Build. Environ. 2008, 43, 1270.
- [9] R. P. Wool, Soft Matter 2008, 4, 400.
- [10] Y. Li, L. Li, J. Sun, Angew. Chem., Int. Ed. 2010, 49, 6129.
- [11] T.-S. Wong, S. H. Kang, S. K. Tang, E. J. Smythe, B. D. Hatton, A. Grinthal, J. Aizenberg, *Nature* 2011, 477, 443.
- [12] S. A. Odom, S. Chayanupatkul, B. J. Blaiszik, O. Zhao, A. C. Jackson, P. V. Braun, N. R. Sottos, S. R. White, J. S. Moore, Adv. Mater. 2012, 24, 2578.
- [13] S. R. White, N. R. Sottos, P. H. Geubelle, J. S. Moore, M. R. Kessler, S. R. Sriram, E. N. Brown, S. Viswanathan, *Nature* 2001, 409, 794.
- [14] E. N. Brown, N. R. Sottos, S. R. White, Exp. Mech. 2002, 42, 372.
- [15] E. N. Brown, S. R. White, N. R. Sottos, Compos. Sci. Technol. 2005, 65, 2474.
- [16] K. S. Toohey, N. R. Sottos, J. A. Lewis, J. S. Moore, S. R. White, Nat. Mater. 2007, 6, 581.
- [17] S. D. Bergman, F. Wudl, J. Mater. Chem. 2008, 18, 41.
- [18] S. Burattini, B. W. Greenland, D. Chappell, H. M. Colquhoun, W. Hayes, Chem. Soc. Rev. 2010, 39, 1973.
- [19] E. B. Murphy, F. Wudl, Prog. Polym. Sci. 2010, 35, 223.

- [20] R. J. Wojtecki, M. A. Meador, S. J. Rowan, Nat. Mater. 2011, 10, 14.
- [21] P. Song, H. Wang, Adv. Mater. 2020, 32, 1901244.
- [22] P. Song, Z. Xu, Y. Lu, Q. Guo, Macromolecules 2015, 48, 3957.
- [23] B. J. Adzima, C. J. Kloxin, C. N. Bowman, Adv. Mater. 2010, 22, 2784.
- [24] S. Burattini, H. M. Colquhoun, B. W. Greenland, W. Hayes, Faraday Discuss. 2009, 143, 251.
- [25] S. Burattini, B. W. Greenland, W. Hayes, M. E. Mackay, S. J. Rowan, H. M. Colquhoun, Chem. Mater. 2011, 23, 6.
- [26] S. Burattini, B. W. Greenland, D. H. Merino, W. Weng, J. Seppala, H. M. Colquhoun, W. Hayes, M. E. Mackay, I. W. Hamley, S. J. Rowan, J. Am. Chem. Soc. 2010, 132, 12051.
- [27] J. Fox, J. J. Wie, B. W. Greenland, S. Burattini, W. Hayes, H. M. Colquhoun, M. E. Mackay, S. J. Rowan, J. Am. Chem. Soc. 2012, 134, 5362.
- [28] L. R. Hart, J. H. Hunter, N. A. Nguyen, J. L. Harries, B. W. Greenland, M. E. Mackay, H. M. Colquhoun, W. Hayes, *Polym. Chem.* 2014, 5, 3680.
- [29] S. Coulibaly, A. Roulin, S. Balog, M. V. Biyani, E. J. Foster, S. J. Rowan, G. L. Fiore, C. Weder, *Macromolecules* 2014, 47, 152.
- [30] Z. Wang, M. W. Urban, Polym. Chem. 2013, 4, 4897.
- [31] H. Zhang, D. Han, Q. Yan, D. Fortin, H. Xia, Y. Zhao, J. Mater. Chem. A 2014, 2, 13373.
- [32] Y. Chen, A. M. Kushner, G. A. Williams, Z. Guan, Nat. Chem. 2012, 4, 467.
- [33] D. Montarnal, M. Capelot, F. Tournilhac, L. Leibler, Science 2011, 334, 965.
- [34] X. Liu, C. Lu, X. Wu, X. Zhang, J. Mater. Chem. A 2017, 5, 9824.
- [35] P. F. Cao, B. Li, T. Hong, J. Townsend, Z. Qiang, K. Xing, K. D. Vogiatzis, Y. Wang, J. W. Mays, A. P. Sokolov, Adv. Funct. Mater. 2018, 28, 1800741.
- [36] X. Kuang, K. Chen, C. K. Dunn, J. Wu, V. C. Li, H. J. Qi, ACS Appl. Mater. Interfaces 2018, 10, 7381.
- [37] Y. Lai, X. Kuang, P. Zhu, M. Huang, X. Dong, D. Wang, Adv. Mater. 2018, 30, 1802556.
- [38] Y. Pan, J. Hu, Z. Yang, L. Tan, ACS Appl. Polym. Mater. 2019, 1, 425.
- [39] L. Zhang, Z. Liu, X. Wu, Q. Guan, S. Chen, L. Sun, Y. Guo, S. Wang, J. Song, E. M. Jeffries, Adv. Mater. 2019, 31, 1901402.
- [40] H. Li, S. Thanneeru, L. Jin, C. J. Guild, J. He, Polym. Chem. 2016, 7, 4824.
- [41] J. Chen, J. Liu, T. Thundat, H. Zeng, ACS Appl. Mater. Interfaces 2019. 11, 18720.
- [42] X. Chen, L. Yin, J. Lv, A. J. Gross, M. Le, N. G. Gutierrez, Y. Li, I. Jeerapan, F. Giroud, A. Berezovska, Adv. Funct. Mater. 2019, 29, 1905785
- [43] C. Wang, C. Wang, Z. Huang, S. Xu, Adv. Mater. 2018, 30, 1801368.
- [44] D. Aubrey, S. Ginosatis, J. Adhes. 1981, 12, 189.
- [45] Y. Zhang, S. Wang, X. Li, J. A. Fan, S. Xu, Y. M. Song, K. J. Choi, W. H. Yeo, W. Lee, S. N. Nazaar, Adv. Funct. Mater. 2014, 24, 2028.
- [46] A. Feula, X. Tang, I. Giannakopoulos, A. M. Chippindale, I. W. Hamley, F. Greco, C. Paul Buckley, C. R. Siviour, W. Hayes, Chem. Sci. 2016, 7, 4291.
- [47] A. Faghihnejad, K. E. Feldman, J. Yu, M. V. Tirrell, J. N. Israelachvili, C. J. Hawker, E. J. Kramer, H. Zeng, Adv. Funct. Mater. 2014, 24, 2322
- [48] G. O. Wilson, M. M. Caruso, S. R. Schelkopf, N. R. Sottos, S. R. White, J. S. Moore, ACS Appl. Mater. Interfaces 2011, 3, 3072.
- [49] R. P. Sijbesma, F. H. Beijer, L. Brunsveld, B. J. Folmer, J. K. Hirschberg, R. F. Lange, J. K. Lowe, E. Meijer, Science 1997, 278, 1601.
- [50] X. Chen, C. E. Zawaski, G. A. Spiering, B. Liu, C. M. Orsino, R. B. Moore, C. B. Williams, T. E. Long, ACS Appl. Mater. Interfaces 2020, 12, 32006.
- [51] Q. Zhang, C.-Y. Shi, D.-H. Qu, Y.-T. Long, B. L. Feringa, H. Tian, Sci. Adv. 2018, 4, eaat8192.





- [52] H. Guo, X. Fang, L. Zhang, J. Sun, ACS Appl. Mater. Interfaces 2019, 11, 33356
- [53] Y. Zhuo, V. Håkonsen, Z. He, S. Xiao, J. He, Z. Zhang, ACS Appl. Mater. Interfaces 2018, 10, 11972.
- [54] D. Son, J. Kang, O. Vardoulis, Y. Kim, N. Matsuhisa, J. Y. Oh, J. W. To, J. Mun, T. Katsumata, Y. Liu, Nat. Nanotechnol. 2018, 13, 1057.
- [55] Y.-L. Rao, A. Chortos, R. Pfattner, F. Lissel, Y.-C. Chiu, V. Feig, J. Xu, T. Kurosawa, X. Gu, C. Wang, J. Am. Chem. Soc. 2016, 138, 6020.
- [56] M. Moretti, D. Wendt, D. Schaefer, M. Jakob, E. B. Hunziker, M. Heberer, I. Martin, J. Biomech. 2005, 38, 1846.
- [57] J. Bobyn, G. Wilson, D. MacGregor, R. Pilliar, G. Weatherly, J. Biomed. Mater. Res. 1982, 16, 571.
- [58] P. P. Matloka, J. C. Sworen, F. Zuluaga, K. B. Wagener, *Macromol. Chem. Phys.* 2005, 206, 218.
- [59] R. Keshavaraj, R. W. Tock, Polym.-Plast. Technol. Eng. 1993, 32, 579.
- [60] R. Takahashi, T. Narayanan, S.-I. Yusa, T. Sato, Macromolecules 2018, 51, 3654.
- [61] M. Alauhdin, T. M. Bennett, G. He, S. P. Bassett, G. Portale, W. Bras, D. Hermida-Merino, S. M. Howdle, *Polym. Chem.* 2019, 10, 860
- [62] S. Mani, M. F. Malone, H. H. Winter, J. Rheol. 1992, 36, 1625.
- [63] S. Zheng, Y. Hu, Q. Guo, J. Wei, Colloid Polym. Sci. 1996, 274, 410.

- [64] D. Zhu, Q. Ye, X. Lu, Q. Lu, Polym. Chem. 2015, 6, 5086.
- [65] U. Lafont, H. Van Zeijl, S. Van Der Zwaag, ACS Appl. Mater. Interfaces 2012, 4, 6280.
- [66] S. H. Boura, M. Peikari, A. Ashrafi, M. Samadzadeh, Prog. Org. Coat. 2012, 75, 292.
- [67] Y. Wang, F. Huang, X. Chen, X.-W. Wang, W.-B. Zhang, J. Peng, J. Li, M. Zhai, Chem. Mater. 2018, 30, 4289.
- [68] M.-C. Luo, J. Zeng, X. Fu, G. Huang, J. Wu, Polymer 2016, 106, 21.
- [69] H. Guo, Y. Han, W. Zhao, J. Yang, L. Zhang, Nat. Commun. 2020, 11,
- [70] B. C. Tee, C. Wang, R. Allen, Z. Bao, Nat. Nanotechnol. 2012, 7, 825.
- [71] K. Zhang, G. B. Fahs, E. Margaretta, A. G. Hudson, R. B. Moore, T. E. Long, J. Adhes. 2019, 95, 146.
- [72] H. B. Xu, J. H. Kim, S. Kim, H. J. Hwang, D. Maurya, D. Choi, C.-Y. Kang, H.-C. Song, *Nano Energy* 2019, 62, 144.
- [73] M. Tang, P. Zheng, K. Wang, Y. Qin, Y. Jiang, Y. Cheng, Z. Li, L. Wu, J. Mater. Chem. A 2019, 7, 27278.
- [74] S. Kaur, A. Narayanan, S. Dalvi, Q. Liu, A. Joy, A. Dhinojwala, ACS Cent. Sci. 2018, 4, 1420.
- [75] N. Sato, A. Murata, T. Fujie, S. Takeoka, Soft Matter 2016, 12, 9202.
- [76] A. D. Zimon, Adhesion of Dust and Powder, Springer, New York 2012.
- [77] A. Attia, F. Lehmann, M. Kern, Dent. Mater. 2011, 27, 207.